RSC Advances

ROYAL SOCIETY OF CHEMISTRY

www.rsc.org/advances

Removal of methyl violet dye by adsorption onto *N*-benzyltriazole derivatized dextran

Eunae Cho[a], Muhammad Nazi Tahir[b], Hwanhee Kim[c], Jae-Hyuk Yu[d], Seunho Jung[c,*]

[a] *Institute for ubiquitous information technology and applications (UBITA), Konkuk University, Seoul 143-701, South Korea*

[b]*The Danish Polymer Centre, Department of Chemical and Biochemical Engineering Danmarks Tekniske Universitet (DTU), 2880 Kgs. Lyngby, Denmark*

[c]*Department of Bioscience and Biotechnology, Bio/Molecular Informatics Center & Institute of Ubiquitous Information Technology and Applications (CBRU), Konkuk University, 1 Hwayangdong, Gwangjin-gu, Seoul 143-701, South Korea*

[d]*Departments of Bacteriology and Genetics, University of Wisconsin, Madison, Wisconsin 53706, USA*

*** Corresponding author**

Seunho Jung, Ph. D.

Mailing address: **Professor, Department of Bioscience and Biotechnology, Bio/Molecular Informatics Center & Center for Biotechnology Research** in UBITA, Konkuk University, 1 Hwayang-dong Gwangjin-gu, Seoul 143-701. South Korea

Tel: 82-2-450-3520; fax: 82-2-452-3611; e-mail: shjung@konkuk.ac.kr

Abstract

In this work, *N*-benzyltriazole derivatized dextran was evaluated for its potential as a novel carbohydrate-based adsorbent for the removal of methyl violet dye from water. The modified dextran was synthesized by a click reaction of pentynyl dextran and benzyl azide, and the structure was characterized with nuclear magnetic resonance spectroscopy, elemental analysis, and scanning electron microscopy. Dextran was substituted with a triazole-linked benzyl group. For decolorization of dyeing effluent, adsorption is a very effective treatment; here, the driving force is based on hydrogen bonding, pi stacking, and electrostatic interaction between the methyl violet dye and the *N*-benzyltriazole derivatized dextran. Batch experiments were carried out to investigate the required contact time and the effects of pH, initial dye concentrations, and temperature. The experimental data were analyzed with equilibrium isotherms including the Langmuir, Freundlich, and Temkin models. Based on the Langmuir isotherm, the maximum adsorption capacity was determined to be 95.24 mg of dye per gram of the adsorbent. The adsorption obeyed pseudo-second order kinetics, and a negative $\Delta G°$ value indicated spontaneous adsorption in nature.

Keywords

Methyl violet; Dye removal; Adsorption; *N*-benzyltriazole derivatized dextran; Click reaction.

1.Introduction

Dyes are widely used in textile and paper industries; however, their effluents cause environmental pollution [1]. Since dyes partially block transmission of sunlight into water, they can inhibit the photosynthesis of aquatic plants and the growth of bacteria [2]. Therefore, color is considered to be one obvious indicator of water pollution. Due to their high solubility in water, the removal of dyes is difficult to achieve by conventional physicochemical and biological treatment methods. Methyl violet is a member of a group of basic dyes, are highly visible even at very low concentrations. Since it is also mutagen and mitotic poison, much attention has been paid to developing remediation procedures for methyl violet pollution [3, 4]. Although various dye removal methods have been reported in the literature, such as chemical- and photo-oxidation [5], biological treatment [6], coagulation [7], and adsorption, adsorption has particular advantages: no remaining toxic fragments are left behind, it has flexibility and simplicity of design, and it is a highly effective, easy, and low-cost method. Activated carbon is the most common material used to remove dye by adsorption but it is expensive and requires reactivation of the carbon [8, 9]; inorganic compounds such as alum, polyaluminum chloride, and silica gel present their own environmental problems [10]. Therefore, the development of eco-friendly polysaccharide-based adsorbents would be of great importance. Although chitosan and its derivatives have been investigated for use in the removal of several acidic dyes [11, 12], there has been no report on the use of modified dextran for the removal of toxic dyes from water.

Dextrans are extracellular polysaccharides of varying lengths (M_r 3-2000000), synthesized from sucrose by *Leuconostoc mesenteroides* [13]. The general structure of dextrans consists of a linear backbone of repeating α-1,6-linked $_D$-glucopyranosyl units branched with α-1,2, α-1,3, and α-1,4 linkages, and is viscoelastic in water [14]. Since dextrans are non-toxic, biocompatible, and inert in physiological conditions, they have been targeted for use in some industrial fields, such as food, cosmetics, and pharmaceuticals [15, 16]. To further the potential applications of dextrans, it is possible to modify their hydroxyl groups with specific substituents; for instance, cross-linked and carboxymethyl- and diethylaminoethyl-derivatized dextrans have been utilized as chromatographic separation resins [17].

In the present study, dextrans were modified with a benzyltriazole moiety and explored as functional biopolymers for the methyl violet dye removal. In biomedical science, click chemistry has been used for DNA conjugation and the synthesis of microcapsules and glycopolymers [18]. In this case, the triazole formed is stable

against reduction, hydrolysis, and oxidation. Given the physicochemical properties of the hydrophobic-functionalized dextran, we investigated it for use in the adsorption of methyl violet. The driving force of the adsorption process is considered as non-covalent bonds including hydrogen bonds, hydrophobic effects, π-stacking interactions, and electrostatic interactions as well as the backbone structure of the polymer. Furthermore, the effects of the contact time, initial dye concentration, initial solution pH, and reaction temperature are presented and discussed. Equilibrium isotherms were analyzed according to the Langmuir, Freundlich, and Temkin equations. A pseudo-second order kinetic model and thermodynamic parameters have been determined.

2. Experimental

2.1. Chemicals

Methyl violet 2B and dextran (M_r ~500000, from *Leuconostoc* sp.) were purchased from Fluka analytical and Sigma–Aldrich Co, respectively. Diethyl ether (99.5%) from J.T.Baker and dimethyl sulfoxide (DMSO, 99.9%) from Sigma–Aldrich Co. were used as organic solvents. All other chemicals used were of analytical reagent grade.

2.2. Synthesis of dimsyl lithium

A basic agent, dimsyl lithium ($CH_3SOCH_2^-Li^+$) introduced by Hakomori [19], was prepared as follows. In a round bottom flask dried by heating under nitrogen, 1.6 M methyllithium in diethyl ether was added to an equal volume of DMSO. The mixture was stirred under nitrogen for 90 min, and the freshly prepared dimsyl lithium was used immediately.

2.3. Synthesis of O-(N-benzyl-[1,2,3]-triazoyl)-propyl dextran via a click reaction of pentynyl dextran with benzyl azide

Pentynyl dextran was synthesized using dimsyl lithium, 5-chloro-1-pentyne, and dextran as previously described [20]. Pentynyl dextran (5 g) was dissolved in DMSO/H_2O (4:1 v/v, 150 mL). After dissolution, benzyl azide (2 equiv. per alkynyl group) was added, followed by a freshly prepared 1 M aqueous solution of sodium L-ascorbate (20 mol % per alkynyl group) and $CuSO_4 \cdot 5H_2O$ (5 mol % per alkynyl group). The reaction mixture

was stirred at room temperature for 96 h [21]. The product was dialyzed (molecular weight cutoff (MWCO) > 10000) against deionized water and the final solution was lyophilized.

2.4. Preparation of succinoglycan and N-benzyltriazole derivatized succinoglycan

As an acidic polysaccharide, succinoglycan was isolated and purified from *Sinorhizobium meliloti* [22]. ***N*-**benzyltriazole derivatized succinoglycan was synthesized by the same protocol described in section 2.3 [23].

2.5. Nuclear magnetic resonance (NMR) spectroscopy

A Bruker Avance 500 spectrometer was used to record ^{1}H–NMR spectra. The samples were dissolved in d_6-DMSO at room temperature.

2.6. Scanning electron microscopy (SEM)

To fix the samples on a brass stub, double-sided adhesive carbon tape was used. The samples were coated with a thin gold layer at 30 W for 30 s in a vacuum. SEM images were acquired using a 20 kV accelerating voltage on a JSM-6380 (Jeol, Japan) scanning electron microscope.

2.7 Fourier-transform Infrared (FT-IR) Spectroscopy

FT-IR Spectra were obtained in potassium bromide matrix by using Bruker IFS-66 spectrometer (AMX, Germany). The spectra were recorded in the scanning range was 400–4000 cm^{-1}.

2.8. Intraparticle diffusion study

The possibility of intra-particle diffusion resistance affecting adsorption was explored by using the intraparticle diffusion model as:

$$q_t = k_{id}\, t^{1/2} + C \quad (1)$$

where k_{id} (mg/g· $min^{1/2}$) is the intraparticle diffusion rate constant and C (mg/g) is the boundary layer thickness [24].

2.9. Activation energy and thermodynamics of adsorption

Using an Arrhenius plot [25], the Arrhenius energy of activation (E_a) can be calculated as follows:

$$\ln k_2 = \ln A - E_a/RT \quad (2)$$

where A and R refer to the Arrhenius frequency factor and the gas constant respectively.

Using Eyring's equation (3), the enthalpy ($\Delta H^{\#}$) and entropy ($\Delta S^{\#}$) of activation were calculated from the slope and intercept, respectively, of a plot of ln (k_2/T) versus $1/T$:

$$\ln k_2/T = \ln (k_B/h) + (\Delta S^{\#}/R) - (\Delta H^{\#}/RT) \quad (3)$$

where k_B and h are the Boltzmann and Planck constants, respectively.

The free energy of activation ($\Delta G^{\#}$) was obtained as follows:

$$\Delta G^{\#} = \Delta H^{\#} - T\Delta S^{\#} \quad (4)$$

The spontaneity of the adsorption process was evaluated by measuring changes in the thermodynamic parameters, namely the free energy change (ΔG^0, kJ/mol), the enthalpy change (ΔH^0, kJ/mol), and the entropy change (ΔS^0, J/mol·K). The values of ΔG^0, ΔH^0, and ΔS^0 were calculated by equations 5 and 6. A plot of ln K_c vs. $1/T$ yields a straight line with $-\Delta H^0/R$ and $\Delta S^0/R$ as its slope and intercept, respectively.

$$\Delta G^0 = -RT \ln K_c \quad (5)$$

$$\ln K_c = \Delta S^0/R - \Delta H^0/RT \quad (6)$$

where K_c, the distribution coefficient of the adsorbate, is equal to q_e/C_e.

3. Results and discussion

3.1. N-benzyltriazole derivatized dextran and its structural analysis

A structural analysis of polysaccharides and information about substituent distribution in their derivatives may offer the most fundamental understanding about the functions and properties of polysaccharides. Dextran and its derivatives have been investigated as the critical polysaccharides for medical and industrial applications [26]. In the present study, we evaluated the prepared *O*-(*N*-benzyl-[1,2,3]-triazoyl)-propyl dextran as a carbohydrate-based adsorbent for the dye removal. *N*-benzyltriazole derivatized dextran was synthesized via a click reaction of pentynyl dextran and benzyl azide. The primary dextran derivative, pentynyl dextran, allowed the introduction of aromaticity in the second reaction step (a copper-catalyzed azide-alkyne cycloaddition). The

resulting *N*-benzyltriazole derivatized dextran was evaluated for the adsorption of methyl violet which has aromatic ring structures with heteroatoms.

N-benzyltriazole derivatized dextran was characterized by NMR, elemental analysis (EA), and SEM. As shown in the ^{1}H NMR spectrum (Fig. 1A), aromatic protons and protons at the 2'-position of the benzyl group had peaks located at 7.29 and 5.49 ppm, respectively. Glucose ring protons appear in the range of 3.00-4.00 ppm, and the hydroxyl protons are visible at 4.46 ppm (OH-2), 4.83 ppm (OH-3), and 4.90 ppm (OH-4). Some signals between 1.00 and 3.00 ppm are due to the resonance from residual pentynyl groups [23]. The EA results of *N*-benzyltriazole derivatized dextran and the parent unsubstituted dextran are summarized in the supporting material, in Table S1. Chemical modifications led to a significant increase in the carbon and nitrogen contents of *N*-benzyltriazole derivatized dextran compared with those of parent dextran. Based on the nitrogen contents, the degree of substitution (DS) value was determined to be 0.56. The spherical morphology of the parent dextran was also changed into an uneven state after modification (Fig. 2A and Fig. S2). These structural analyses indicated that the novel adsorbent of dye, *N*-benzyltriazole derivatized dextran was successfully synthesized.

3.2. Adsorption isotherm analysis

Table 1 summarizes the Langmuir, Freundlich, and Temkin isotherm constants for the adsorption of methyl violet 2B onto *N*-benzyltriazole derivatized dextran. The applicability of the isotherm equation was evaluated through the correlation coefficients, r^2 (Table 1 and Fig. S3). The best fit, with an r^2 value of 0.9815, was obtained from the Langmuir isotherm model. Langmuir adsorption quantitatively describes the formation of an adsorbate monolayer on the outer surface of the adsorbent, after which no further adsorption takes place [27]. The maximum amount of the dye adsorbed from the aqueous solution, q_m, was 95.24 mg/g; the constant associated with the binding energy of the sorption system, K_L, was 0.16 L/mg. Other natural adsorbents such as bagasse fly ash, sugarcane dust, and sunflower seed hull have shown q_m values in the range of 25-93 mg/g for methyl violet adsorption (Table S2) [3, 4, 28]. These agricultural materials are localized, and their structural information in the literature is deficient. In these respects, modified polysaccharides can be developed with advantage, and applied for the conventional methods of dye removal from water. The separation factor, R_L, calculated from the Langmuir constant, indicates the nature of the isotherm. The values of R_L in the present

184 investigation were found to range from 0.286 to 0.032 for initial dye concentrations ranging from 10 to 200 ppm
185 (Fig. S4). Higher R_L values at lower dye concentrations showed that the adsorption was more favorable at lower
186 initial adsorbate concentrations; however, all of the R_L values indicate favorable adsorptions, as they all lie in
187 the range of $0 < R_L < 1$. This favorable adsorption may be attributed to van der Waals forces and hydrogen
188 bonding between methyl violet 2B and *N*-benzyltriazole derivatized dextran, as well as π-π interactions between
189 the aromatic residues of the dye and the adsorbent.

190 Freundlich adsorption isotherms are commonly used to describe the adsorption characteristics of
191 heterogeneous surfaces. The extent of adsorption varies directly depending on the pressure until the saturation
192 pressure is reached. The constant K_f and n are the empirical parameters which must be determined by data
193 fitting [29]. The constant K_f is a rough indicator of the adsorption capacity, and 1/n is the adsorption intensity.
194 Chemical adsorption is expected if $1/n < 1$, while if $n = 1$, the partition between the two phases is independent of
195 the concentration, and $1/n > 1$ indicates that the adsorption is a favorable physical process [30]. Therefore, the 1/n
196 value of 2.77 suggests that the adsorption of methyl violet 2B onto *N*-benzyltriazole derivatized dextran is a
197 favorable physical process.

198 Temkin's adsorption isotherm model takes into account the adsorbate/adsorbent interaction, and
199 assumes that the heat of adsorption of all molecules in the layer will decrease linearly with increased surface
200 coverage [31]. It predicts a uniform distribution of binding energies over the whole population of surface binding
201 sites. Theoretically, such a uniform distribution of binding energies would arise from a truly random
202 arrangement of surface binding sites. According to the Temkin plot of adsorption data collected in this
203 experiment ($r^2 = 0.9433$), the constants were calculated as $A_T = 1.37$ L/g and $B = 22.73$ J/mol. Since the heat of
204 sorption lower than 20 kJ/mol is characteristics for physisorption [32].
205
206 ***3.3. Effect of initial dye concentration on methyl violet 2B removal***

207 The effect of the initial dye concentration on its subsequent removal was studied (Fig. 3). The
208 experiments were performed at different initial dye concentrations (12.5, 25, and 50 ppm) with *N*-benzyltriazole
209 derivatized dextran acting as the adsorbent (1 g/L). In the case of the initial concentration of 12.5 ppm, 89% of
210 the dye was removed from water at 25 °C within 30 min. At a 50 ppm initial dye concentration, 57% was
211 removed after 2 h. Using the graph shown in Fig. 3B, the rate constants of the pseudo-second order, k_2 (g/mg

min), and amounts of dye adsorbed at equilibrium, q_e (mg/g), were determined to be: k_2 = 0.0515 (12.5 ppm), 0.0271 (25 ppm), and 0.0042 (50 ppm); q_e = 11.05 (12.5 ppm), 23.47 (25 ppm), 30.21 (50 ppm). At a low initial concentration, the adsorption of dye by the adsorbent is very intense and reaches equilibrium very quickly. For the diffusion mechanism, the kinetic results were further analyzed by the intraparticle diffusion model. Fig. 3C shows plots of q_t vs. $t^{1/2}$ at different initial dye concentration, and they are presented as at least two linear graphs. The results indicate that two or more steps simultaneously operate the adsorption process [33]. In addition, the presence of intercept implies that the intraparticle diffusion is not the only rate-limiting step [34]. The first portion represents boundary layer diffusion through the bulk liquid to the external surface of the adsorbent. The second linear phase is a gradual adsorption stage through the intraparticle diffusion. The intraparticle diffusion rate constants were calculated as: K_{id} (mg/g·min$^{1/2}$) = 0.1274 (12.5 ppm), 0.1372 (25 ppm), and 1.0389 (50 ppm). Therefore, we suggest that both surface adsorption and intraparticle diffusion affect the present adsorption mechanism.

3.4. Comparison with N-benzyltriazole derivatized succinoglycan

Considering that methyl violet 2B is a basic dye (Fig. 4A), it is meaningful to investigate the contribution of acidic groups to its adsorption. Since succinoglycan is an anionic glucan containing succinyl and pyruvyl substituents [22], *N*-benzyltriazole derivatized succinoglycan was prepared via a click reaction for the comparison with *N*-benzyltriazole derivatized dextran. Figs. 4B and 4C show the unmistakable effectiveness of *N*-benzyltriazole derivatized dextran as an adsorbent for the removal of methyl violet, with residual color less than 5%. Parent dextran showed a better result than the unmodified succinoglycan, and *N*-benzyltriazole derivatized succinoglycan gave a removal improvement of 30% over unmodified succinoglycan. In a previous study, the removal of another class of organic contaminant, polycyclic aromatic hydrocarbons (PAH), was attributed to the exposed aromatic cores in the modified pine bark [35]. The aromatic cores resulted in a stronger specific π-π interaction between the PAH and the adsorbent. Based on the EA of the tested polysaccharides (Table S1), the values of (N+O)/C indicating polarity, decreased after modification from 0.96 and 0.92 to 0.50 and 0.50 for succinoglycan and dextran, respectively. The aliphatic character (H/C) of each also decreased from 2.06 and 1.98 to 1.46 and 1.37, respectively. Thus, aromaticity is not the only deciding factor for adsorption; the polysaccharide backbone structure is also important.

As another key, the surface morphology of *N*-benzyltriazole derivatized dextran, with its roughness, supports the effective adsorption of dye (Fig. 2A). The craterous surface structure of *N*-benzyltriazole derivatized dextran may allow methyl violet 2B to be trapped and adsorbed into its holes [36]. Conversely, *N*-benzyltriazole derivatized succinoglycan shows a laminar sheet-like surface [23], and parent dextran has a spherical structure with the average diameter of 20.03 μm (Fig. S2). In reality, the uneven surface of the *N*-benzyltriazole derivatized dextran was filled after the adsorption of dye, as shown in Fig. 2B. Morphological changes were also observed for the adsorption by other adsorbents [4, 37]. From the plot profiles of the selected 50 μm line in the SEM data (according to Fiji image processing package), the 8 potholes of 2-5 μm width and the flattened surface are described in blue and red line, respectively (Fig. 2C). The gray scale can be considered as an underestimation due to the image treatment software effect, however the degree of surface roughness is clearly differentiated. These results indicate that various non-covalent bonds including π-π interaction and its uneven surface work at the present dye adsorption.

3.5. FT-IR spectra of N-benzyltriazole derivatized dextran/methyl violet 2B composite

After adsorption methyl violet 2B onto *N*-benzyltriazole derivatized dextran, the precipitated composite was analyzed with FT-IR spectroscopy. Fig. 5 shows shifts or changes of IR absorption peaks, indicating interactions of the adsorbent and methyl violet. All the observed changes are summarized in Table S3, and the characteristic change is present at C≡C and aromatic C=C stretching vibration. A disappearance in the C≡C stretch may be attributed to the electrostatic interaction of tertiary ammonium ion of methyl violet with the terminal alkyne group of *N*-benzyltriazole derivatized dextran (Fig. 1). A novel peak (1587 cm^{-1}) belong to methyl violet 2B was formed, and band shifts took place from 1643 to 1637 cm^{-1}. This result demonstrates the additional function of residual alkyne group in *N*-benzyltriazole derivatized dextran for electrostatic interaction with methyl violet. Similar observations have also been reported in methylene blue/exfoliated graphene oxide composite [38].

3.6. Effect of pH on methyl violet 2B removal

Adsorption processes are affected by solution pH, as it influences not only the surface charge of the adsorbent but also the chemistry of dye in solution [39]. We depict the effect of pH on dye removal by *N*-

benzyltriazole derivatized dextran (Fig. 6); we found that the dye adsorption decreased as the pH increased. Under alkaline condition, the hydrogen bonds stabilizing the adsorbate-adsorbent interaction can be destroyed, and the *N*-benzyltriazole derivatized dextran may adopt another conformation because of charge repulsion. Whereas the opposite trend was observed in the adsorption of basic dye onto sunflower seed hull and bagasse fly ash [3, 4].

3.7. Effect of temperature, activation energy, and a thermodynamic study

The adsorption studies were carried out at different temperatures, ranging from 15 to 75 °C (Table 2 and Fig. S5). The adsorption capacity and the rate constant were found to increase with increasing temperature, indicating that the adsorption is an endothermic process. This may be due to an increase in the mobility of the dye or a change of active sites within the internal structure of the *N*-benzyltriazole derivatized dextran as the temperature increases. The present dye adsorption follows the pseudo-second order model with the best correlation coefficient ($r^2 > 0.99$); using the rate constant for pseudo-second order adsorption (k_2) at several temperatures, the energy of activation (E_a) was calculated to be 33.96 kJ/mol from an Arrhenius plot (Fig. S6A and Table 2). In general, activation energies less than 40 kJ/mol indicate a physisorption process, while those higher than 40 kJ/mol signify chemisorption [40]. Thus, the present adsorption of methyl violet 2B by *N* -benzyltriazole derivatized dextran can be regarded as predominantly physisorption.

Table 3 shows thermodynamic parameters as obtained from the intercept and slope of a plot of ln K_c vs. $1/T$ (Fig. S7). The positive $\Delta H°$ value, 16.47 kJ/mol, also indicates that the adsorption is an endothermic process; furthermore, the magnitude of this value provides information about the type of sorption. In principle, the heat evolved during physical adsorption is of the same order of magnitude as the heat of condensation, i.e., 2.1-20.9 kJ/mol, while the heat of chemisorption generally falls in the range of 80-200 kJ/mol [41]. Although the low value of $\Delta S°$ implies that no remarkable change in entropy occurred during adsorption, the positive value may be attributed to an increased randomness at the solid-solution interface during adsorption. The negative values of $\Delta G°$ (-3.90, -5.61, and -6.71 kJ/mol) at the given temperatures (288, 308, and 328 K) indicate that the adsorption processes at all three recorded temperatures are spontaneous.

4. Conclusion

In the present study, *N*-benzyltriazole derivatized dextran was successfully synthesized by a click reaction. It was then evaluated for its effectiveness as a polysaccharide adsorbent for the removal of methyl violet dye from water. Equilibrium and kinetic studies were carried out for the adsorption of methyl violet onto *N*-benzyltriazole derivatized dextran. The monolayer adsorption capacity was determined to be 95.24 mg of dye per gram of *N*-benzyltriazole derivatized dextran. The adsorption efficiency was found to be dependent on the initial dye concentration, solution pH, adsorbate contact time, and temperature. The adsorption kinetics followed a pseudo-second order model. A thermodynamic study supported the theory that the adsorption of methyl violet 2B onto *N*-benzyltriazole derivatized dextran is a spontaneous and endothermic process at the studied temperatures. We suggest that methyl violet removal by *N*-benzyltriazole derivatized dextran is caused by physical adsorption based on hydrogen bonding, van der Waals interactions, and π-stacking interactions, and electrostatic interactions. The present study indicates great potential for the removal of cationic dyes from aqueous solutions using natural biomaterials. Furthermore, the practical use of tailor made polysaccharide-derivative adsorbents to remove various dye and organic pollutants as target chemicals could be expected in the environmental field.

Acknowledgements

This paper was supported by the KU Research Professor Program of Konkuk University. This research was also supported by the National Research Foundation of Korea Grant, funded by the Korean Government (NRF-2013R1A1A2012568 and NRF-2011-619-E0002), and by the Priority Research Centers Program through the National Research Foundation of Korea (NRF), funded by the Ministry of Education, Science, and Technology (2012-0006686). SDG.

References

1. Y. Anjaneyulu, N. S. Chary and D. S. S. Raj, *Reviews in Environmental Science and Bio/Technology*, 2005, **4**, 245-273.
2. N. Koprivanac and H. Kusic, *Hazardous organic pollutants in colored wastewaters*, Nova Science Publishers Hauppauge, 2009.
3. I. D. Mall, V. C. Srivastava and N. K. Agarwal, *Dyes and pigments*, 2006, **69**, 210-223.
4. B. Hameed, *Journal of hazardous materials*, 2008, **154**, 204-212.
5. M. S. Lucas and J. A. Peres, *Dyes and Pigments*, 2006, **71**, 236-244.
6. H. S. Rai, M. S. Bhattacharyya, J. Singh, T. Bansal, P. Vats and U. Banerjee, *Critical Reviews in Environmental Science and Technology*, 2005, **35**, 219-238.
7. B. Shi, G. Li, D. Wang, C. Feng and H. Tang, *Journal of Hazardous Materials*, 2007, **143**, 567-574.
8. Y. S. Al-Degs, M. I. El-Barghouthi, A. H. El-Sheikh and G. M. Walker, *Dyes and Pigments*, 2008, **77**, 16-23.
9. G. Walker and L. Weatherley, *Water Research*, 1997, **31**, 2093-2101.
10. S. Lambert, N. Graham, C. Sollars and G. Fowler, *Water science and technology*, 1997, **36**, 173-180.
11. V. Dhanapal and K. Subramanian, *Carbohydrate polymers*, 2014.
12. G. Crini and P.-M. Badot, *Progress in polymer science*, 2008, **33**, 399-447.
13. A. Jeanes, C. A. Wilham and J. C. Miers, *The Journal of biological chemistry*, 1948, **176**, 603-615.
14. A. Misaki, M. Torii, T. Sawai and I. J. Goldstein, *Carbohydrate research*, 1980, **84**, 273-285.
15. M. Naessens, A. Cerdobbel, W. Soetaert and E. J. Vandamme, *Journal of Chemical Technology and Biotechnology*, 2005, **80**, 845-860.
16. R. Mehvar, *Journal of controlled release*, 2000, **69**, 1-25.
17. B. Porsch and L.-O. Sundelöf, *Journal of Chromatography A*, 1994, **669**, 21-30.
18. K. Nwe and M. W. Brechbiel, *Cancer Biotherapy and Radiopharmaceuticals*, 2009, **24**, 289-302.
19. S.-I. HAKOMORI, *Journal of Biochemistry*, 1964, **55**, 205-208.
20. M. N. Tahir, C. Bork, A. Risberg, J. C. Horst, C. Komoß, A. Vollmer and P. Mischnick, *Macromolecular Chemistry and Physics*, 2010, **211**, 1648-1662.

21. P. F. Tankam, P. Mischnick, H. Hopf and P. G. Jones, *Carbohydrate research*, 2007, **342**, 2031-2048.
22. L.-X. Wang, Y. Wang, B. Pellock and G. C. Walker, *Journal of bacteriology*, 1999, **181**, 6788-6796.
23. E. Cho, K. Kim, M. N. Tahir, J. Y. Lee and S. Jung, *Notes*, 2014, **35**, 2589.
24. W. Weber and J. Morris, *J. Sanit. Eng. Div. Am. Soc. Civ. Eng*, 1963, **89**, 31-60.
25. J. W. Grissom, T. L. Calkins, H. A. McMillen and Y. Jiang, *The Journal of organic chemistry*, 1994, **59**, 5833-5835.
26. D. de Belder, *Polysaccharides in Medicinal Applications. New York, NY: Marcel Dekker*, 1996, 505-524.
27. I. Langmuir, *Journal of the American Chemical Society*, 1918, **40**, 1361-1403.
28. Y.-S. Ho, W.-T. Chiu and C.-C. Wang, *Bioresource technology*, 2005, **96**, 1285-1291.
29. A. Akgerman and M. Zardkoohi, *Journal of Chemical & Engineering Data*, 1996, **41**, 185-187.
30. S. V. Mohan and J. Karthikeyan, *Environmental pollution*, 1997, **97**, 183-187.
31. R. D. Johnson and F. H. Arnold, *Biochimica et Biophysica Acta (BBA)-Protein Structure and Molecular Enzymology*, 1995, **1247**, 293-297.
32. P. Atkins, Oxford University Press, 1998.
33. L. Ai, M. Li and L. Li, *Journal of Chemical & Engineering Data*, 2011, **56**, 3475-3483.
34. S. Ghorai, A. Sarkar, M. Raoufi, A. B. Panda, H. Schönherr and S. Pal, *ACS applied materials & interfaces*, 2014, **6**, 4766-4777.
35. Y. Li, B. Chen and L. Zhu, *Bioresource technology*, 2010, **101**, 7307-7313.
36. H. L. Parker, A. J. Hunt, V. L. Budarin, P. S. Shuttleworth, K. L. Miller and J. H. Clark, *RSC Advances*, 2012, **2**, 8992-8997.
37. S. Dawood and T. K. Sen, *Water research*, 2012, **46**, 1933-1946.
38. G. Ramesha, A. V. Kumara, H. Muralidhara and S. Sampath, *Journal of colloid and interface science*, 2011, **361**, 270-277.
39. N. M. Mahmoodi, B. Hayati, M. Arami and C. Lan, *Desalination*, 2011, **268**, 117-125.
40. T. Anirudhan and P. Radhakrishnan, *The Journal of Chemical Thermodynamics*, 2008, **40**, 702-709.
41. Y. Liu and Y.-J. Liu, *Separation and Purification Technology*, 2008, **61**, 229-242.

Figure Legends

Fig. 1. ^{1}H-NMR spectra of (A) *O*-(*N*-benzyl-[1,2,3]-triazoyl)-propyl dextran and (B) dextran. The left insets show the chemical structures of *N*-benzyltriazole derivatized dextran and dextran.

Fig. 2. SEM images of (A) *N*-benzyltriazole derivatized dextran and (B) *N*-benzyltriazole derivatized dextran with dye adsorbed. (C) Plot profiles of the selected yellow line (blue line : *N*-benzyltriazole derivatized dextran; red line : *N*-benzyltriazole derivatized dextran with dye adsorbed). Black arrows indicate the gap width.

Fig. 3. (A) The effect of initial dye concentration. (B) Pseudo-second order kinetic plots on the removal of methyl violet 2B by adsorption onto *N*-benzyltriazole derivatized dextran. (C) Intraparticle diffusion plots for the adsorption of methyl violet onto *N*-benzyltriazole derivatized dextran. (25 °C; 1g/L adsorbent)

Fig. 4. (A) The chemical structure of methyl violet 2B. (B) Color changes and (C) degree of residual color after reaching adsorption equilibrium. Polysaccharide adsorbents: a, no addition; b, succinoglycan; c, *N*-benzyltriazole derivatized succinoglycan; d, dextran; e, *N*-benzyltriazole derivatized dextran. (10 g/L adsorbent)

Fig. 5. FT-IR spectra of *N*-benzyltriazole derivatized dextran before (in red) and after adsorption (in blue).

Fig. 6. Effect of pH on dye removal by *N*-benzyltriazole derivatized dextran. (100 ppm dye, 10 g/L adsorbent; buffers used: pH 2, HCl-KCl buffer; pH 4, citrate buffer; pH 7, phosphate buffer; pH 9, borate buffer; pH 10, $NaHCO_3$·NaOH buffer; pH 11, $NaHCO_3$·NaOH buffer)

Tables and Figures

Table 1. Isotherm constants for methyl violet adsorption onto *N*-benzyltriazole derivatized dextran at 25 °C. (Adsorbent dose: 5g/L)

Langmuir isotherm constant		
K_L **(L/mg)**	q_m **(mg/g)**	r^2
0.16	95.24	0.9815
Freundlich isotherm constant		
K_f **(mg/g)**	***n***	r^2
16.04	0.36	0.9787
Temkin isotherm constant		
B **(J/mol)**	A_T **(L/g)**	r^2
22.73	1.37	0.9433

Table 2. Activation parameters for dye adsorption onto *N*-benzyltriazole derivatized dextran. (25 ppm dye; 1g/L adsorbent)

Temperature (°C)	k_2 **(mg/g min)**	E_a **(kJ/mol)**	r^2	$\Delta H^{\#}$ **(kJ/mol)**	$\Delta S^{\#}$ **(J/mol K)**	$\Delta G^{\#}$ **(kJ/mol)**	r^2
15	0.0031					84.19	
35	0.0068					87.86	
45	0.0148	33.96	0.9602	31.33	-183.548	89.70	0.9531
55	0.0221					91.53	
75	0.0310					95.20	

411 **Table 3.** Thermodynamic parameters of dye adsorption onto *N*-benzyltriazole derivatized dextran. (25 ppm dye;
412 1g/L adsorbent)

413

Temperature (K)	K_c	$\Delta G°$ (kJ/mol)	$\Delta H°$ (kJ/mol)	$\Delta S°$ (J/mol·K)	r^2
288	1.6293	-3.8993			
308	2.1905	-5.6067	16.4677	71.0308	0.9746
328	2.4629	-6.7130			

414

415

Fig. 1.

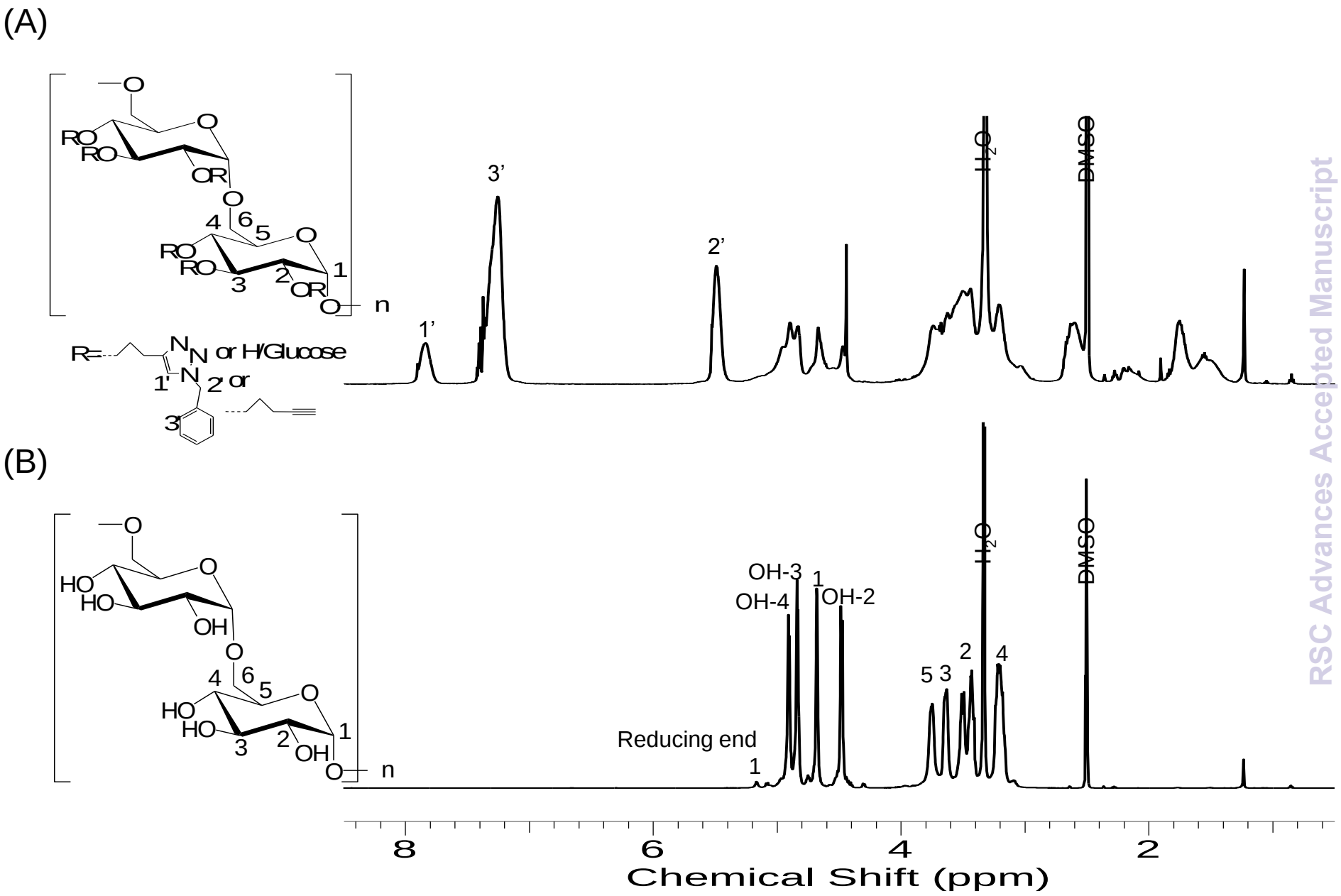

Fig. 2.

(A)

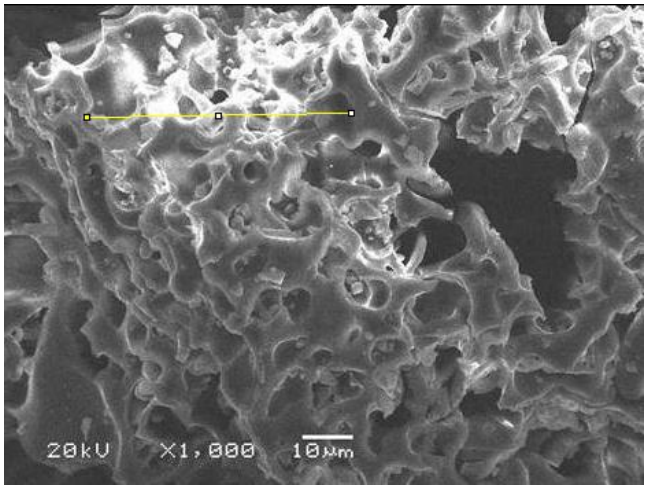

(B)

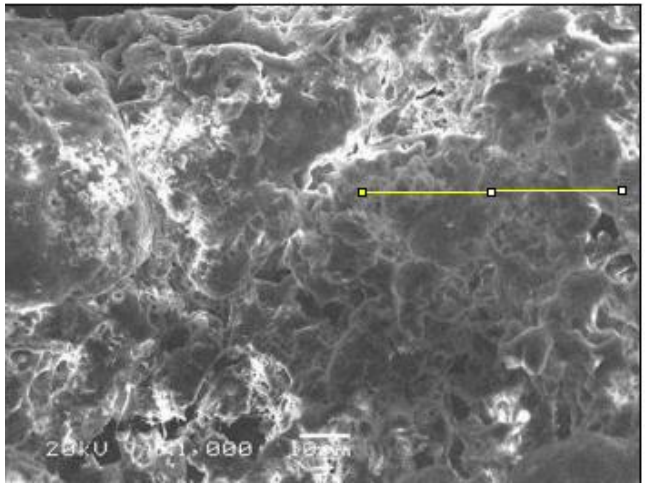

(C)

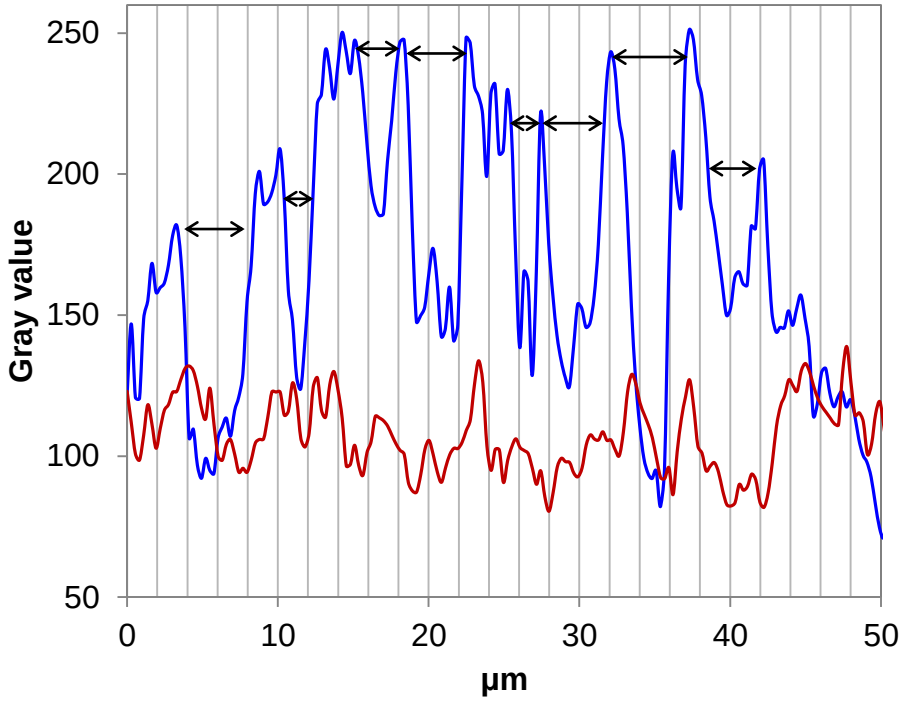

Fig. 3.

(A)

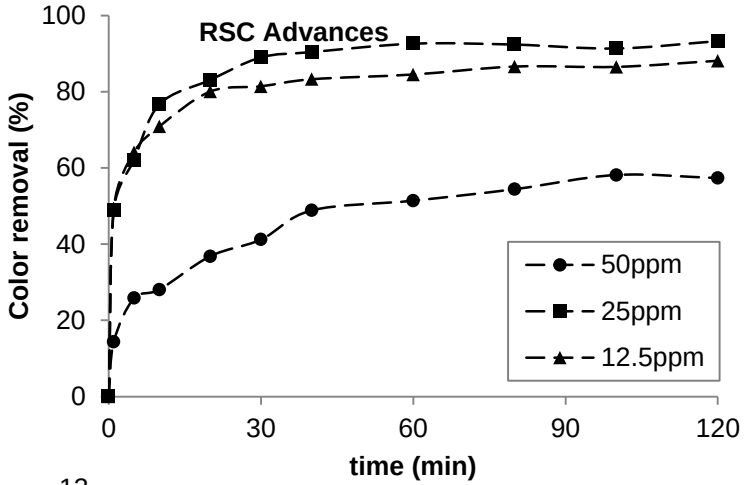

(B)

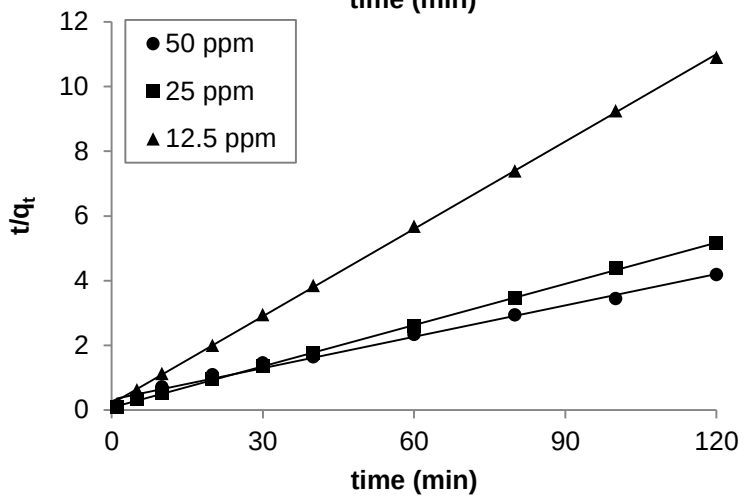

(C)

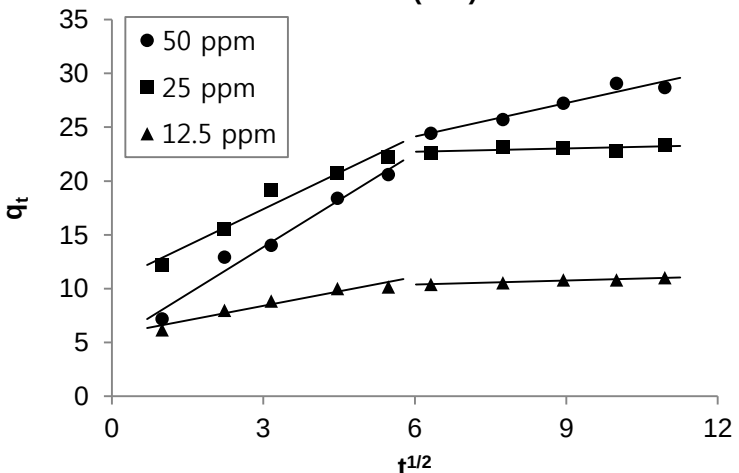

Fig. 4.

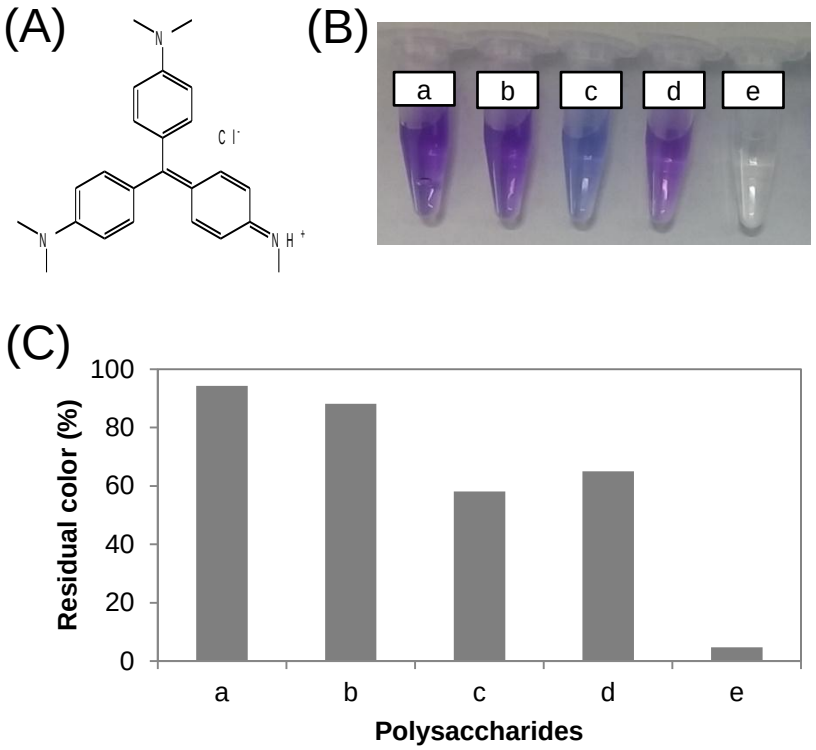

Fig. 5.

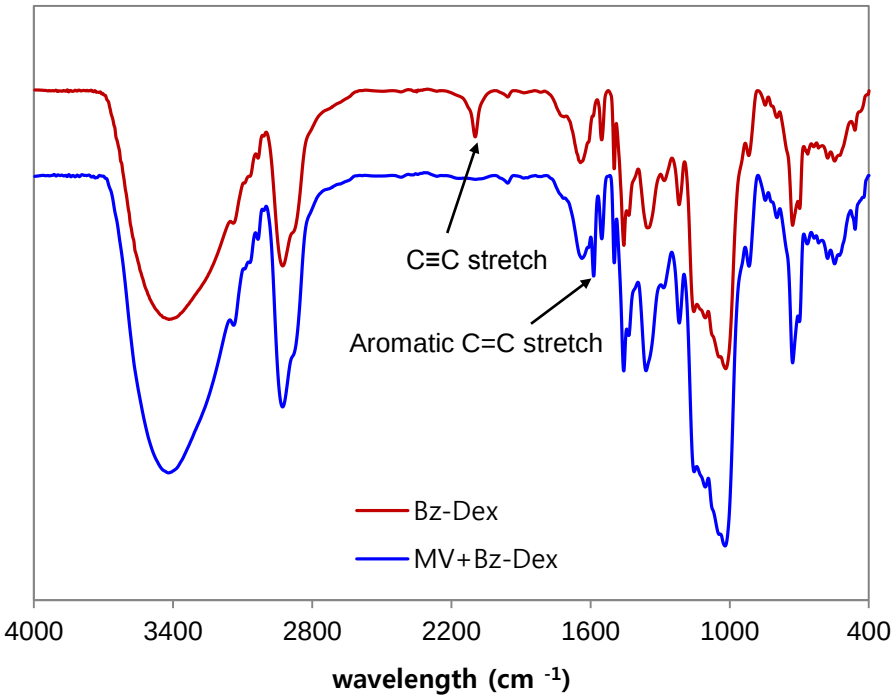

Fig. 6.